Mesenchymal Stem Cell Carriers Protect Oncolytic Measles Viruses from Antibody Neutralization in an Orthotopic Ovarian Cancer Therapy Model

Emily K. Mader,[1] Yoshihiro Maeyama,[1] Yi Lin,[2] Greg W. Butler,[2] Holly M. Russell,[1] Evanthia Galanis,[1] Stephen J. Russell,[1] Allan B. Dietz,[2] and Kah-Whye Peng[1]

Abstract

Purpose: Preexisting antiviral antibodies in cancer patients can quickly neutralize oncolytic measles virus (MV) and decrease its antitumor potency. In contrast to "naked" viruses, cell-associated viruses are protected from antibody neutralization. Hence, we hypothesized that measles virotherapy of ovarian cancer in measles-immune mice might be superior if MV-infected mesenchymal stem cell (MSC) carriers are used.

Experimental Design: Antimeasles antibodies titers in ovarian cancer patients were determined. The protection of MV by MSC from antimeasles antibodies, the *in vivo* biodistribution profiles, and tumor infiltration capability of MSC were determined. Measles-naïve or immune tumor–bearing mice were treated with naked virus or MSC-associated virus and mice survivals were compared.

Results: MSC transferred MV infection to target cells via cell-to-cell heterofusion and induced syncytia formation in the presence of high titers of antimeasles antibody, at levels that completely inactivated naked virus. Athymic mice bearing i.p. human SKOV3ip.1 ovarian tumor xenografts passively immunized with measles-immune human serum were treated with saline, naked MV, or MV-infected MSC. Bioluminescent and fluorescent imaging data indicated that i.p. administered MSC localized to peritoneal tumors, infiltrated into the tumor parenchyma, and transferred virus infection to tumors in measles naïve and passively immunized mice. Survival of the measles-immune mice was significantly enhanced by treatment with MV-infected MSC. In contrast, survivals of passively immunized mice were not prolonged by treatment with naked virus or uninfected MSC.

Conclusions: MSC should be used as carriers of MV for intraperitoneal virotherapy in measles-immune ovarian cancer patients. (Clin Cancer Res 2009;15(23):7246–55)

Epithelial ovarian cancer is the most lethal of all gynecologic malignancies, killing >15,000 women in the United States each year (1). Due to the lack of effective screening modalities, the majority of patients present with advanced stage III disease at the time of diagnosis where the cancer still remains confined within the peritoneal cavity (2). Primary treatment is maximal debulking surgery followed by chemotherapy using carboplatin and paclitaxel or carboplatin alone (3). More than 75% of patients will eventually relapse, and salvage therapies for recurrent disease are not curative. Various novel biological therapeutics are being developed for the treatment of ovarian cancer; these include immunotherapy using tumor vaccines, monoclonal antibody (Ab) therapy, gene transfer of cytotoxic and antiangiogenic transgenes, and virotherapy using replication-competent tumor selective viruses (4–8).

We have been developing the Edmonston vaccine lineage of MV as a tumor selective oncolytic agent for cancer therapy (9). Oncolytic MV uses the hemagglutinin envelope glycoprotein to infect cancer cells via the cellular CD46 receptor and the fusion envelope glycoprotein to trigger fusion of the viral cell membranes for virus entry (10). Expression of these fusogenic hemagglutinin and fusion proteins on surfaces of virus-infected cells results in massive intercellular fusion with uninfected neighboring CD46-positive cells to generate the characteristic measles virus (MV)–induced cytopathic effects (CPE) of syncytia formation (11). We recently showed that overexpression of CD46 on cell surfaces results in the preferential killing of tumor cells (12, 13). Indeed, human ovarian cancer cells overexpress CD46 (14) and are highly susceptible to measles-induced CPE and cell killing (10, 12).

A phase I dose escalation clinical trial testing the safety of i.p. administration of 10^3 to 10^9 $TCID_{50}$ of MV-CEA, a recombinant MV genetically modified to express a soluble marker

Authors' Affiliations: [1]Department of Molecular Medicine and [2]Divisions of Transfusion Medicine and Laboratory Medicine, Mayo Clinic, Rochester, Minnesota

Received 5/20/09; revised 8/19/09; accepted 9/8/09; published OnlineFirst 11/24/09.

Grant support: The Minnesota Ovarian Cancer Alliance, Andersen Foundation, Alliance for Cancer Gene Therapy, and the National Cancer Institute (CA136547 and CA129966).

The costs of publication of this article were defrayed in part by the payment of page charges. This article must therefore be hereby marked *advertisement* in accordance with 18 U.S.C. Section 1734 solely to indicate this fact.

Requests for reprints: Kah-Whye Peng, Guggenheim 18, Mayo Clinic, 200 First Street Southwest, Rochester, MN 55905. Phone: 507-284-8357; Fax: 507-284-8388; E-mail: peng.kah@mayo.edu.

doi:10.1158/1078-0432.CCR-09-1292

Translational Relevance

Recombinant oncolytic measles viruses (MV) derived from the Edmonston vaccine lineage are undergoing phase I clinical testing in cancer patients. Although results from a recently completed trial testing i.p. administration of MV-CEA in patients with recurrent ovarian cancer indicated that MV-CEA was well tolerated, it is also apparent that virotherapy was suboptimal in these measles-immune patients. Here, we showed that human MSC could protect MV from neutralization by antiviral antibodies and serve as carriers to deliver MV to ovarian tumors. I.p. administered MSC trafficked to and colocalized with orthotopic OVCAR5, A2780, and SKOV3ip.1 human ovarian tumor xenografts in mice, enhancing contact of virus with the tumors. In addition, virus-loaded MSC transferred MV infection efficiently to ovarian tumor xenografts and significantly extended the survival of mice passively immunized with antimeasles antibodies. Cell carriers should be incorporated in clinical trials using MV in ovarian cancer patients.

peptide to enable noninvasive monitoring of the profiles of viral gene expression, was recently completed (10, 15). The virus was well tolerated, and no dose-limiting toxicity was observed. There were, however, early indications of biological activity, especially in patients treated with higher doses of MV-CEA (16). As a possible follow-up trial using MV in ovarian cancer patients, we are exploring various strategies to improve delivery of MV to the tumor site, especially in patients with preexisting anti-measles antibodies. We and others have reported that cells can potentially be used as carriers to deliver oncolytic viruses to tumor xenografts in murine models, although only one study has evaluated the therapeutic activity of cell carriers given (intratumorally) to mice with preexisting antiviral antibodies (17–22). Potentially, any cell can be used as a virus carrier; for example, irradiated cell lines (20, 23), cytokine-induced killer cells (18), activated T cells (21), mesenchymal stem cell (MSC; ref. 24), and CD14+ monocyte–derived dendritic cells (25). MSCs are attractive as cell carriers because, in addition to their reported ability to home to tumors (26), adipose tissue–derived MSC are readily obtained from adipose tissues that are available as surgical wastes from gastric bypass or from fat biopsies. MSC can be expanded to large numbers in cellular therapy laboratories of medical centers under Good Laboratory Practice conditions, and clinical experience with infusion of MSC into humans is available (27). Here, we have chosen to test adipose tissue–derived MSC as a MV carrier in mice bearing orthotopic human ovarian tumor xenografts, focusing on their potential to overcome antiviral immunity in mice passively immunized with antimeasles antisera.

Materials and Methods

Viruses, lentivectors, and cell lines. Recombinant Edmonston strain MV expressing firefly luciferase (FLuc), red fluorescent protein (RFP), green fluorescent protein (GFP), and sodium iodide symporter (NIS) were generated as described previously (28, 29). Viral titers were determined by $TCID_{50}$ titration on Vero cells. To generate the lentivectors, 293T cells were cotransfected with gag-pol expression plasmid pCMV8.91, VSV.G envelope expression plasmid pMD-G, and vector plasmid encoding Gaussia luciferase with an IRES linking cyan fluorescent protein (a kind gift from Dr. Bakhos A Tannous, Harvard Medical School, Cambridge, MA; refs. 30, 31). Vector supernatant was collected 48 h later, filtered (0.45 μm) and frozen at -80°C. Human ovarian cancer cells, SKOV3ip.1, stably expressing GLuc were maintained in α MEM (Lonza) that was supplemented with 20% fetal bovine serum (FBS, Life Technologies), 100 U/mL penicillin-streptomycin, and 2 mmol/L L-glutamine. Human ovarian cancer cell lines A2780 and OVCAR5 (kind gift from Dr. Viji Shridhar, Mayo Clinic, Rochester, MN) were maintained in 10% fetal bovine serum-DMEM. Adipose-derived MSC were maintained in Advanced MEM (Invitrogen) that was supplemented with 5% platelet lysate, 2 U/mL heparin, 100 U/mL penicillin-streptomycin, and 2 mmol/L L-glutamine. All media and growth supplements were purchased from Invitrogen.

Generation and characterization of MSC. Adipose tissue–derived MSC were generated as described. Briefly, fat tissue was mechanically dissected and disaggregated, cells were pelleted by centrifugation and left to adhere to plastic wells in media supplemented with a 5% solution of lysed human platelets. Typical cell recovery was $1.3 + 0.68 \times 10^6$ cells/g of tissue ($n = 7$). These cells were phenotyped for typical MSC cell markers, and were negative for Class II, CD14, CD45, CD106, and positive for CD44, CD49d, CD71, CD73, CD90, CD105, CD166, and Class I.[3] Phenotype of cells remained stable for more than seven passages and after cryopreservation. Cells were frozen in aliquots in liquid nitrogen and stored until use. Only low-passage cells (P5-7) were used for all the experiments of this study.

Virus infection assays. MSC were plated overnight in 6- or 12-well plates and MV-RFP at various multiplicities of infection (MOI, ratio of virus to cells) for 2 h at 37°C, after which the virus inoculum was removed, and the cells were cultured for 48 h in the presence or absence of a fusion inhibitory peptide (FIP, Z-D-Phe-Phe-Gly-OH; Bachem). Cells were trypsinized and the percentage of red fluorescent MV-RFP–infected cells was determined by flow cytometry. Numbers of viable cells were determined by trypan blue exclusion assay at various time points post infection.

Measles-immune human serum. Pooled human AB sera were purchased from Valley Biomedical, Inc. The antimeasles Ab (IgG) titers of the sera were determined by the Mayo Clinic Serology Clinical Laboratory (Diamedix enzyme immunoassay). Antimeasles Ab titers are reported as EU/mL. The corresponding full plaque reduction neutralization (PRN) titers of the sera were also determined (see below).

Virus neutralization assays. For the virus neutralization assays, ascites or sera were heat inactivated and diluted in Opti-MEM (2-fold serial dilutions) after which 100 to 250 $TCID_{50}$/50 μL MV-GFP was added. The mixture was incubated at 37°C for 30 min after which Vero cells (7×10^3 cells/well/50 μL) were added and the mixture was plated in 96-well plates. The culture was maintained at 37°C for 2 d. Each dilution was done in triplicates, and the presence or absence of CPE in the wells was noted. The full PRN titer is the reciprocal of the highest dilution at which no CPE was noted in any of the replicate wells and before the dilution where CPE was observed in one or more wells.

Immunohistochemical staining for MV-N and CD68 proteins. Tumors were sectioned into halves and frozen immediately in optimal cutting temperature medium. Cryosections (5 μm thick) were acetone fixed for 10 min. The cryosections were permeabilized using 0.01% Triton X-100 and 5% horse serum for 15 min and incubated with biotinylated anti-MV nucleocapsid (MV-N) protein Ab (Mab 8906, Chemicon) for 1 h. The slides were developed using Vector ABC and alkaline phosphatase substrate kits (Vector Laboratories) and counterstained with Vector Nuclear Fast Red. For CD68 staining, acetone-fixed cryosections were incubated with biotinylated rat antimouse CD68

[3] A. Dietz, unpublished data.

(Serotec) for 1 h. The slides were developed using Vector Elite ABC and DAB substrate kits (Vector Laboratories) and counterstained with Vector Hematoxylin QS.

In vivo *experiments*. All procedures involving animals were approved by and performed according to guidelines of the Institutional Animal Care and Use Committee of Mayo Foundation. To determine the half-life of human anti-measles Ab postpassive transfer into mice, athymic mice were given an i.p. injection of PBS-diluted measles-immune human serum. At 3 h (day 0), day 1, 2, 3, 4, 7, and 8 postserum infusion, mice were euthanized and bled, and the level of anti-MV neutralizing Ab titer in murine serum was determined by full PRN assay on Vero cells. The decrease in anti-MV Ab titer was plotted over time.

To establish various orthotopic models of human ovarian cancer, female athymic mice (5-6 wk of age; Taconic Laboratory) were injected i.p. with 2×10^6 SKOV3ip.1 cells stably expressing Gaussia luciferase-cyan fluorescent protein (SKOV3ip.1-Gluc-CFP) or Fluc (SKOV3ip.1-FLuc), OVCAR5 or A2780 cells. Another cohort of tumor-bearing mice also received CellTracker Red CMTPX dye–labeled (red fluorescent) MV-infected MSC. Mice were euthanized, and tumors were harvested and examined using a fluorescence microscope.

For the therapy experiments, MSC were preinfected with MV-NIS (MOI, 4.0) for 2 h, washed in PBS, and exposed to 50 EU of measles-immune serum for 30 min, at 37°C, to ensure complete neutralization of any bound virus. An equivalent amount of cell-free MV-NIS viral stock was also exposed to 50 EU of measles-immune serum for 30 min, at 37°C. At the end of the incubation period, cells or MV-NIS in measles-immune serum were injected i.p. into mice that had received either 50 EU of measles-immune serum (measles immune) or saline (measles naïve) 3 h earlier. Each mouse received 10^5 $TCID_{50}$ MV-NIS or 10^5 infected MSC, diluted in saline or measles-immune serum. Mice were imaged to determine tumor burden (FLuc or GLuc). For imaging, mice were given either i.p. injections of 150 mg/kg D-luciferin (Xenogen) 15 min before imaging for Fluc activity or i.p. injections of 20 mg/kg colenterazine substrate (Nanolight Technology, Prolume Ltd.) 10 min before imaging for GLuc activity. Whole abdominal bioluminescence signals reflecting tumor burden (GLuc) or viral gene expression (FLuc) were quantitated using the Living Image 2.50 software (Xenogen) according to manufacturer's protocol. Mice were euthanized when they developed ascites, and had lost >20% of body weight or could not reach food or water. All remaining mice were euthanized at day 86. Kaplan-Meier survival curves were compared by logrank test in GraphPad Prism (GraphPad Software). *P* values of <0.05 were considered significant.

Table 1. Anti-measles IgG levels (EU/mL) and corresponding virus PRN titers in ascites fluids of ovarian cancer patients (n = 14)

Sample ID	Anti-MV Ab titer	PRN titer
OvCa12	26.10	64
OvCa9	38.40	8
OvCa8	54.30	2
OvCa2	75.70	N.d.
OvCa4	85.70	N.d.
OvCa5	86.00	N.d.
OvCa1	94.50	N.d.
OvCa10	102.80	32
OvCa3	108.00	N.d.
OvCa7	108.00	N.d.
OvCa6	110.00	N.d.
OvCa14	145.80	128
OvCa11	148.50	64
OvCa13	154.40	64

NOTE: A titer of >20 EU/mL is considered measles seropositive.
Abbreviation: N.d., not done.

Results

Ovarian cancer patients have preexisting antimeasles antibodies. Ascites fluid wastes were collected from ovarian cancer patients who came to Mayo Clinic for drainage of their ascites. All clinical samples were obtained with Institutional Review Board approval and patient consent. The cellular fraction was removed and the anti-MV IgG titers in ascites fluids were determined. As shown in Table 1, all ascites fluids tested positive for anti-MV antibodies (anti-MV IgG titers, >20 EU/mL). The average anti-MV IgG titer was 95 + 39 EU/mL (mean + SD, n = 14). The corresponding virus PRN titer of the ascites fluids ranged from 2 to 128 (Table 1).

Infection of MSC by MV. To determine the susceptibility of MSC to MV infection, MSC were infected with MV-RFP at MOI (0.01, 0.1, 1.0, or 4.0). As shown in Fig. 1A, there was a corresponding increase in the numbers of infected cells with increase in MOI. To enable quantitation of the percentage of infected cells by flow cytometry, MSC were maintained in media containing a FIP (+FIP) that prevents intercellular fusion (syncytia formation). At MOI of 1.0 and 4.0, 20% and 60% of cells were expressing RFP by 48 hours postinfection, respectively (Fig. 1B).

Viability of MSC postinfection by MV-GFP (MOI, 1.0) was determined by trypan blue exclusion assay (Fig. 1C). In the presence of FIP, there was no significant difference in numbers of viable cells in the infected culture over time. The numbers of viable cells decreased by 96 hours if the infected MSC were allowed to fuse with neighboring cells in the absence of FIP. The amount of viral progeny produced by infected MSC (cell-associated virus) or conditioned media (released virus) was determined by $TCID_{50}$ titrations. Infected MSC were able to propagate the virus, but to a smaller extent, compared with Vero producer cells (Fig. 1D). The majority of MV progeny was cell associated, requiring freeze/thaw cycles to release the viruses (Fig. 1D).

Intercellular fusion is more resistant to neutralizing anti-MV antibodies than cell-free virus. The anti-MV IgG titers in different lots of human AB pooled sera were determined using an enzyme immunoassay. An individual with a titer of >20 EU/mL is measles immune. Full PRN assays using 250 $TCID_{50}$ MV-GFP were also done to determine the corresponding virus neutralization titers of the sera. Pooled AB serum lot K61552 (277 EU/mL, PRN = 256) and lot C80553 (300 EU/mL, PRN = 256) were used in all subsequent experiments.

Vero cells were infected with MV-GFP (10^3 $TCID_{50}$) in the absence or presence of increasing concentrations of measles-immune serum. The numbers of infectious centers (syncytia) in the Vero monolayer were counted at 48 hours postinfection and represented as a percentage of syncytia count in the absence of anti-MV antibodies. Naked MV-GFP was neutralized by measles-immune sera; no syncytium was detected at the highest concentration of human serum used (1:4 dilution, 69 EU/mL). It was not until at 1:128 serum dilution (2 EU/mL) that 40% of infectious centers was recovered in the Vero monolayer (Fig. 2A).

To determine if MSC could deliver MV to target cells in the presence of anti-MV antibodies, MSC were preinfected with MV-GFP at MOI of 1.0, and the next day, MSC were overlaid on Vero cells (1 MSC: 100 Vero cells) in the presence of increasing concentrations of measles-immune serum. From Fig. 2B, it is apparent that MSC-associated viruses were more resistant to

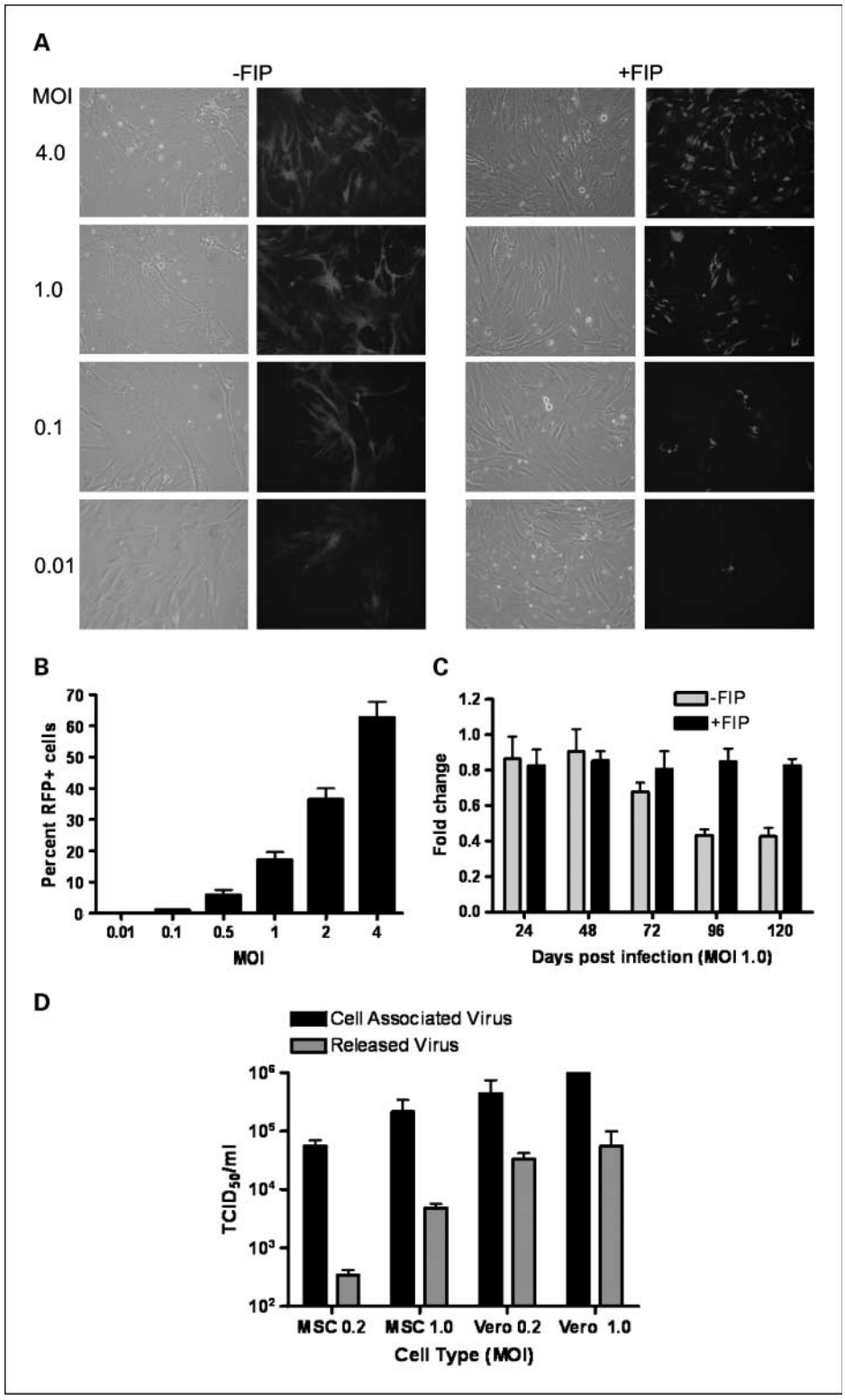

Fig. 1. Adipose tissue–derived MSC are susceptible to infection by MV. *A,* photographs MV-RFP–infected MSC taken at 48 h postinfection using different MOI. Cells were maintained in the absence (*-FIP*) or presence (*+FIP*) of a FIP. *B,* quantitation of MV-RFP infection in MSC by analyzing for numbers of RFP-positive cells (*+FIP*) by flow cytometry at 48 h postinfection. *C,* viability of infected MSC over time. *D,* progeny produced by virus infected MSC or Vero cells at 48 h postinfection at MOI of 0.2 or 1.0. Amount of cell-associated virus or released virus in the supernatant were titrated on Vero cells. Columns, mean (n = 3 replicates); bars, SD.

the neutralizing effects of anti-MV antibodies. At 1:4 serum dilution (69 EU/mL), 40% of infectious centers was present and at 1:16 dilution, the numbers of infectious centers were comparable with the control in which no serum was added. Hence, infected MSC were able to fuse with Vero cells and delivered MV infection to the target cells in an environment with a high amount of anti-MV antibodies.

Localization of MSC post i.p. administration into mice. Athymic mice were implanted i.p. with SKOV3ip.1 human ovarian cancer cells, and 7 d later, mice were injected i.p. with MV-Luc–infected MSC and imaged noninvasively for Fluc gene expression. FLuc signals were seen both in tumor-free and tumor-bearing mice given MV-Luc–infected MSC at day 1 post-MSC delivery (Fig. 3A). In the nontumor-bearing mice (*top*), the MV-Luc–infected cells were seen

at the injection site and at the omental region (highlighted by orange line). By day 3, the luciferase signals had decreased significantly and were undetectable by day 7 after death of the virus-infected MSC cells (Fig. 3A, *top*). In contrast, bioluminescent signals remained high and continued to increase over time in tumor-bearing mice given MV-Luc–infected MSC. It is evident that in tumor-bearing mice, the infected MSC were able to transfer MV-Luc infection to the peritoneal tumors. The infected tumors continued to propagate the virus, resulting in increase of FLuc bioluminescent signal even after death of the infected MSC (Fig. 3A). As expected, naked MV-Luc was highly efficient at infecting tumors in these measles naïve mice (Fig. 3A, *bottom*).

To determine if MSCs colocalized with the tumor nodules, another cohort of mice bearing intraperitoneal SKOV3ip.1, OVCAR5, or A2780 human ovarian tumors were injected i.p. with CellTracker Red CMTPX dye–labeled MSC (MV infected or uninfected). Tumors were harvested and examined directly under a fluorescence microscope 24 hours later. Abundant red fluorescent MSC were found at the omental tumor nodules and on smaller peritoneal tumor nodules that have seeded on the mesenteric linings or intestines (Fig. 3B). There was no apparent difference in the biodistribution of uninfected and infected MSC; both types of MSC were able to traffic to and localize on the tumors. Gross examination of the peritoneal cavity indicated that peritoneal tumor nodules in all three models of ovarian cancer were covered with red fluorescent MSC. In the OVCAR5 model in which there was significant coverage of the peritoneum wall by a cake of tumor cells, abundant MSC were found on the tumor cake (Fig. 3B). In contrast, the tumor-free peritoneal wall next to this tumor cake had minimal numbers of MSC (Fig. 3B). When given i.p. into control athymic mice with no tumor, MSC accumulated predominantly on the omentum (Fig. 3B). Cryosections of the peritoneal tumors were examined using confocal microscopy to determine the extent of MSC infiltration into the tumor parenchyma. At 4 and 24 hours post–cell infusion, red fluorescent MSC were seen lining the surface of the tumor nodules and in the tumor parenchyma (Fig. 3C).

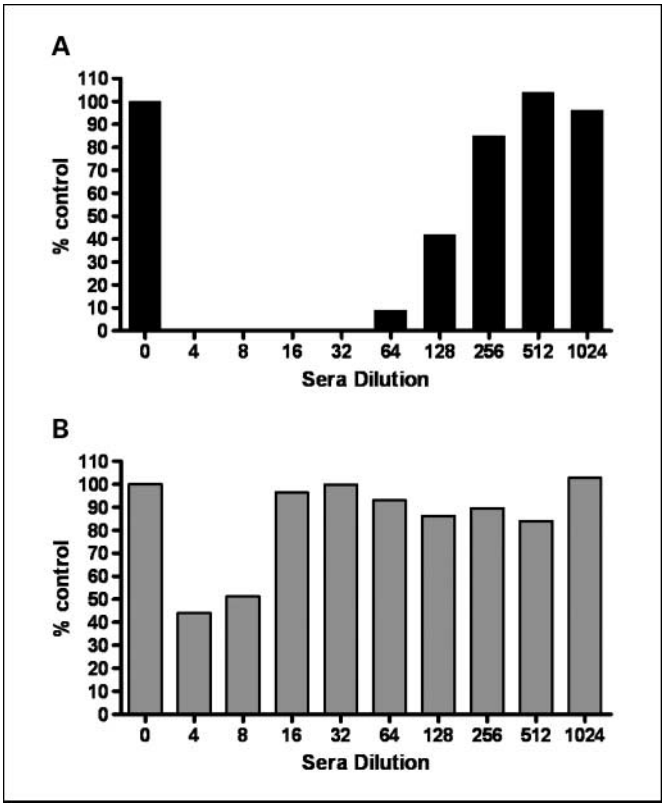

Fig. 2. Virus delivered by infected MSC carriers is more resistant to inhibition by antimeasles antibodies than by cell-free naked virus. *A,* MV-GFP virus was mixed with varying dilutions of human measles-immune sera (1:4 to 1:1024 dilution in 5% fetal bovine serum-DMEM) and added to Vero cells. *B,* MSC were infected with MV-GFP (MOI, 1.0) and the next day, MSC were mixed with varying dilutions of human measles-immune sera and overlaid on Vero cells. The Vero cells were cultured for 2 d and the numbers of syncytia were counted and represented as a percentage of numbers of syncytia found in wells with no serum. A representative experiment from three replicates is shown.

Passive immunization of athymic mice with measles-immune serum. Mice are not susceptible to infection by MV because they lack the CD46 receptor required for virus entry. Measles virus is also unable to replicate in murine tissues due to an intracellular block to transcription of viral genes (32, 33). Thus, we used the passive immunization method in which measles-immune human serum was injected i.p. into mice to generate measles-immune animals. We validated this method by giving athymic mice an i.p. injection of measles-immune human serum and measuring the level of neutralizing anti-MV antibodies present in the mouse sera at different time points. At 3 hours after i.p. injection of human serum (80 EU per mouse), the mice were confirmed to be measles-immune and the full PRN titers of the murine sera ranged between 64 and 512 (Fig. 4A). There was a gradual decrease in the PRN titers over the 1-week time interval. The estimated half-life of neutralizing antimeasles Ab in the mice was 19.2 hours. In all subsequent experiments, virus or cell carrier delivery was done at 3 hours after i.p. infusion of this measles-immune pooled human serum.

Antitumor efficacy in the presence of neutralizing antibodies. Athymic mice were implanted with SKOV3ip.1-GLuc tumor cells, and 8 days later, mice received saline or equal numbers (1×10^6) of naked cell–free MV-Luc or MV-Luc–infected MSC. Mice were imaged noninvasively using bioluminescent imaging for GLuc expression with colenterazine substrate (tumor burden) and, the next day, for Fluc expression using D-luciferin substrate (viral gene expression). Imaging was done 1 day apart to ensure that all Gluc-bioluminescent signals had disappeared before FLuc imaging. We observed a good correlation between the location and intensity of GLuc and FLuc signals (Fig. 4B), indicating robust infection of the tumors by cell-free and MSC-associated virus in measles-naïve animals. In measles-immune animals, the MV-Luc–infected MSC were able to transfer the infection to ovarian tumors, resulting in increase in FLuc signal. In contrast, "naked" MV-Luc was neutralized by the anti-measles antibodies and the peritoneal tumors were not infected (Fig. 4B). Hence, delivery of MV is superior when MSC are used as virus carriers in measles-immune animals. The increase in FLuc signal in the tumors at day 7 was not due to presence of infected MSC. A significant portion of virus-infected MSC died by day 3 after i.p. delivery into mice resulting in complete loss of bioluminescent signals (Fig. 3A).

To investigate the antitumor activity of the various treatments, athymic mice were implanted i.p. with 2×10^6 SKOV3ip.1-GLuc tumor cells, and 8 days later, mice were passively immunized by i.p. administration of measles-immune human serum (50 EU) or given saline. Three hours later, mice were given equal numbers

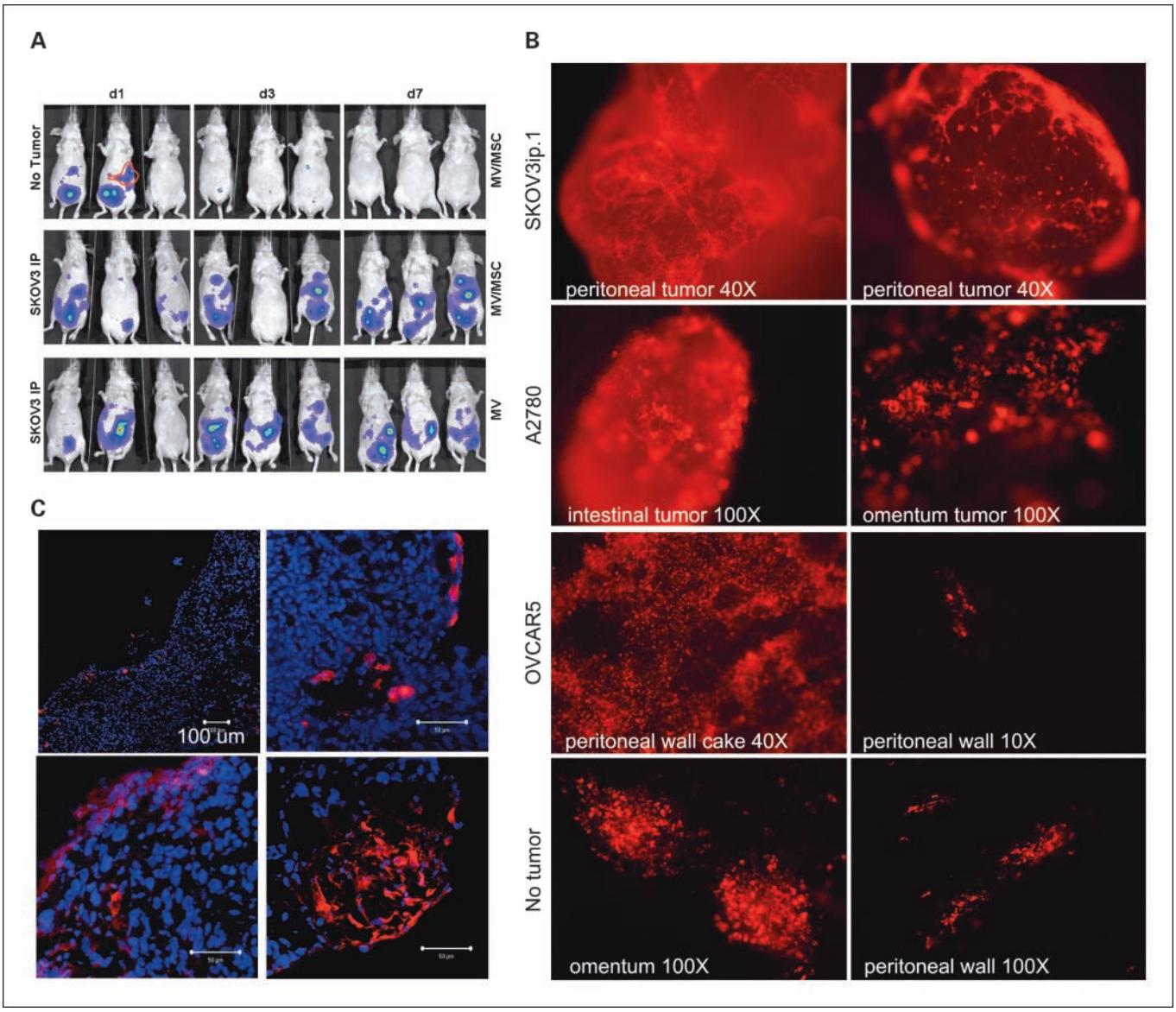

Fig. 3. *In vivo* distribution of MSC after i.p. delivery. *A,* serial bioluminescent imaging of mice after i.p. injection of MV-Luc–infected MSC (*MV/MSC*) into mice with no tumor or mice bearing intraperitoneal human SKOV3ip.1 ovarian tumors. Another group of tumor-bearing mice received MV-Luc (*MV*). *B,* MV-infected MSC were labeled with a fluorescent CellTracker Red CMTPX dye and injected i.p. into mice bearing peritoneal SKOV3ip.1, A2780, or OVCAR5 human ovarian tumors. Mice were euthanized 24 h later. Photographs (×40 or ×100 magnification) of freshly harvested tissues showing red fluorescent MSCs on the omentum or peritoneal wall of mice with no tumor or on the tumor nodules of mice. *C,* confocal microscopy images of tumor cryosections demonstrating presence of red fluorescent MSC on the surface and in the parenchyma of SKOV3ip.1 tumors. Scale bars, 100 μm unless otherwise indicated.

(1×10^5) of cell-free MV-NIS or MV-infected MSC i.p. The MV/MSC had been loaded with MV-NIS by incubation with virus at MOI of 4.0 for 2 hours (~60% infection; Fig. 1) and washed once in PBS. In the measles-immune groups, MV-NIS and MV/MSC were subsequently incubated *in vitro* with measles-immune serum (50 EU) for 30 min at 37°C before injection into the animals to ensure neutralization of any surface-bound virus. Thus, each measles-immune mouse received a total of 100 EU of anti-MV IgG Ab.

The Kaplan Meier survival curves of the mice were plotted (Fig. 5). The median survival for saline control was 31 days (n = 5 mice), uninfected MSC was 31 days (n = 5 mice), MV (-Ab) was 64 days (n = 12 mice), MV (+Ab) was 31 days (n = 12 mice), MV/MSC (-Ab) was 62 days (n = 10 mice), and MV/MSC (+Ab) was 66 days (n = 11 mice). All mice in the saline, uninfected MSC, and MV (+Ab) groups (22 of 22) were euthanized because they developed bloody ascites (3-4.5 mL), with extensive dissemination of ovarian tumors in the peritoneal cavity, perigastric area, and on the peritoneal side of the diaphragm. In contrast, only a few of the mice in the MV (-Ab) or MV/MSC groups (+Ab and - Ab) developed ascites (6 of 33). Several of the mice appeared jaundiced and were euthanized (12 of 33). Examination at necropsy indicated tumor obstruction/constriction around the gall bladder or bile duct. The rest of the animals were euthanized due to weight loss of >20%, or development of an ulcerated subcutaneous tumor at the injection site toward the end of the study.

The survival curves of the respective treatment groups were compared against the saline control and the *P* values were determined (Fig. 5A). Uninfected MSC did not have any antitumor activity against human ovarian cancer, survival of these mice was not significantly different from the saline-treated group ($P = 0.92$). As expected, MV-NIS (-Ab) significantly extended the survival of mice compared with saline control ($P < 0.0001$). However, the antitumor activity of MV-NIS was negated in passively immunized mice. Thus, there was a significant difference in survival outcome using naked MV-NIS in measles-naïve mice versus measles-immune mice ($P < 0.0001$). In contrast to therapy using cell-free virus, treatment of passively immunized mice with MV-infected MSC significantly extended the survival of mice ($P < 0.0001$), doubling the median survival from 31 days (MV-NIS +Ab) to 66 days for MV/MSC +Ab. Furthermore, there was no significant difference in therapy using MV/MSC in measles naïve or measles-immune animals ($P = 0.93$). The presence of preexisting anti-measles antibodies did not diminish the delivery and transfer of MV from infected MSC. We did not observe a significant difference in survival of measles-naïve mice treated with MSC-associated MV compared with cell-free virus ($P = 0.67$).

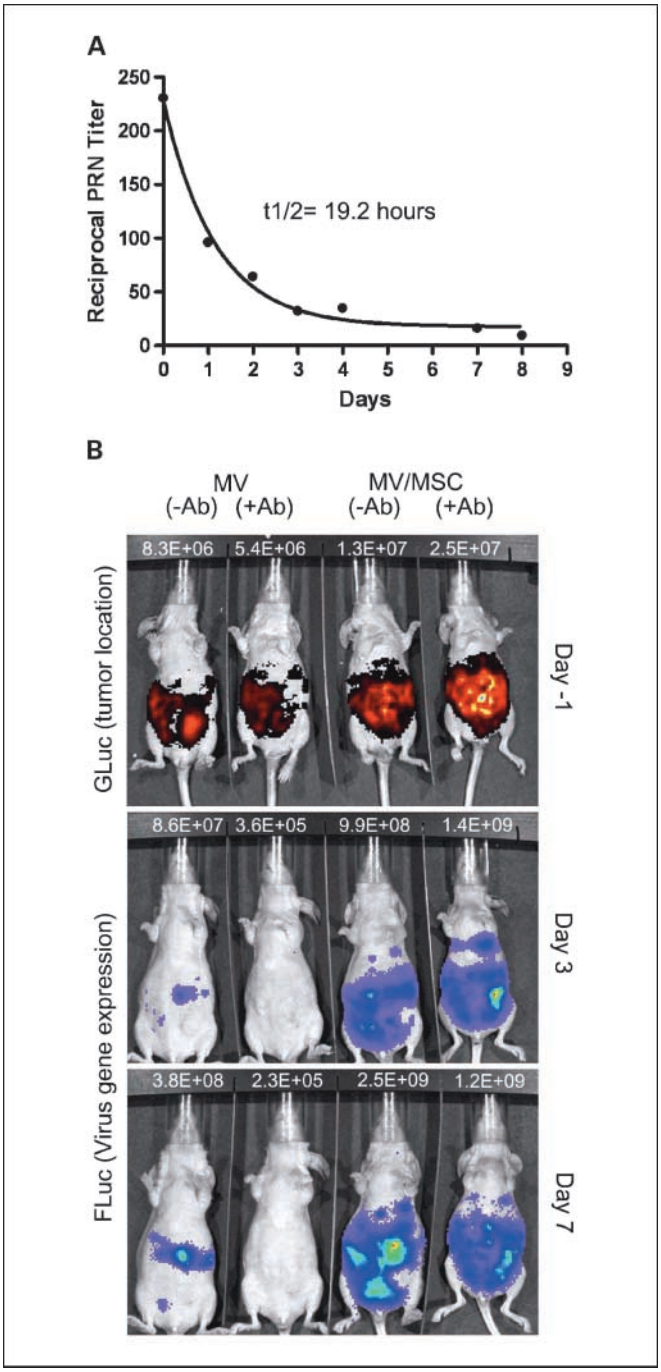

Fig. 4. MSC protect MV from complete neutralization by anti-measles Ab in mice. *A*, timeline for decay of human measles-immune serum in sera of athymic mice over time. Mice were euthanized at each time point to obtain serum for virus PRN assays. Each point is the average of PRN assays from two to four mice. Curve fit $R^2 = 0.99$. *B*, representative photographs showing correlation between tumor location (indicated by GLuc activity) and MV-Luc gene expression (FLuc activity), delivered by cell-free virus or MSC-associated virus in measles-naïve or measles-immune mice. Mice were imaged using colenterazine substrate for GLuc expression 1 d before imaging for FLuc activity using D-luciferin substrate. The photons count (photons/second) for each mouse is as indicated.

Cryosections of omental tumors harvested at necropsy were immunostained with an Ab specific for the measles nucleocapsid (MV-N) protein and CD68, a macrophage marker. As shown in Fig. 5B, MV-N–positive areas were found in MV-NIS (-Ab), MV/MSC (-Ab), and MV/MSC (+Ab) tumors but not in MV-NIS (+Ab) tumors. Staining for CD68+ macrophages indicated abundant infiltration of phagocytic macrophages into the MV-infected tumors, either surrounding or in necrotic areas or colocalizing with the MV-N–positive areas. It is likely that the macrophages are phagocytic in nature, as suggested by the abundance of CD68 staining in the necrotic areas of the tumors (see black arrow in MV/MSC +Ab tumor). There were also areas of MV-N staining with no corresponding CD68 staining (e.g., last panel, MV/MSC +Ab tumor).

Discussion

The Edmonston vaccine strain of MV is capable of inducing tumor-selective destruction of ovarian cancer cells while sparing normal cells in the peritoneal cavity (10, 11). However, many ovarian cancer patients have preexisting anti-measles antibodies. As a strategy to protect oncolytic MV from neutralizing antiviral antibodies and improve delivery of the virus to peritoneal tumors, we evaluated the potential of adipose tissue–derived MSC for delivery of MV to orthotopic human ovarian tumors after i.p. administration in passively immunized mice.

A major potential of advantage of using cells as carriers for delivery of viruses to tumors is protection of the oncolytic virus from antiviral antibodies. In addition, carrier cells can also interact dynamically with the host by responding to chemokines secreted by tumors and may preferentially accumulate at tumor sites. In contrast, systemically administered viruses are sequestered rapidly by the reticuloendothelial system of the liver and spleen and become unavailable for circulation to the tumor. Virus-infected cells may also serve as *in situ* virus production factories, thereby increasing the numbers of infectious virus available in the tumor microenvironment. The "ideal" cell carrier should be susceptible to virus infection or be able to "carry" the virus on/in the cell, remain viable for a sufficient period of time postinfection to transfer the virus, and be able to support virus replication/progeny production (19, 21, 34). However, there are also disadvantages associated with cell

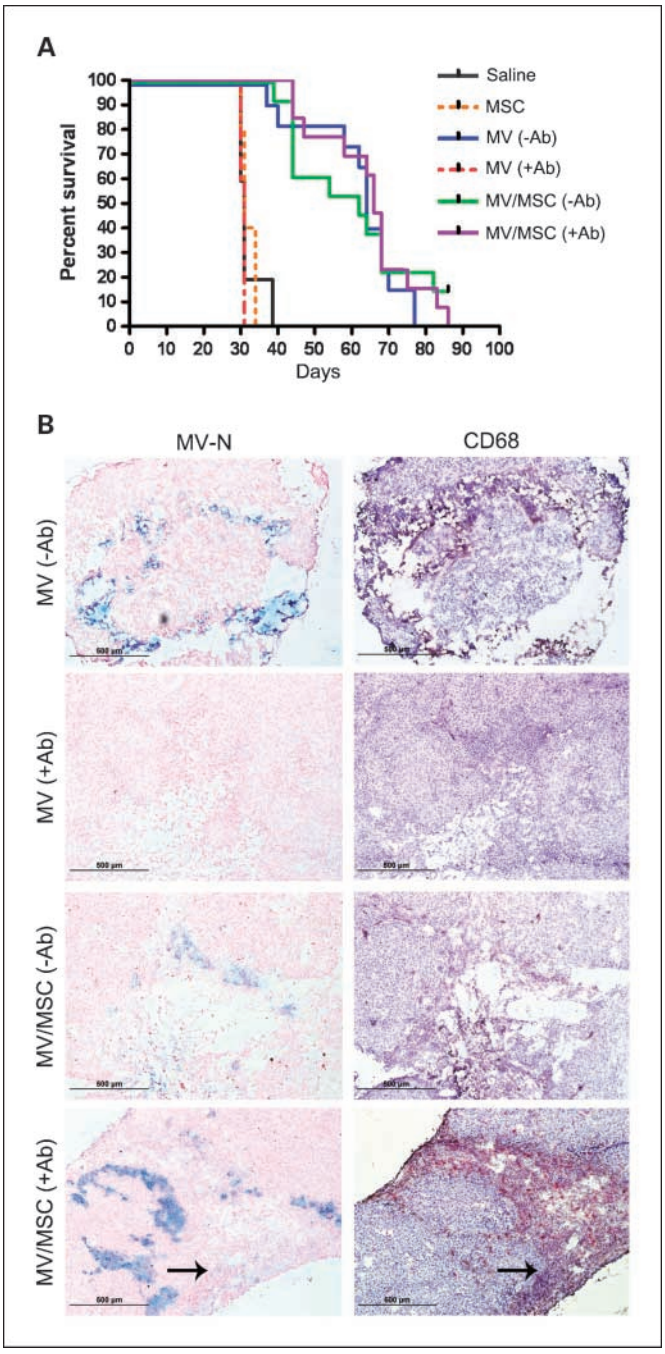

Fig. 5. MSC-mediated delivery of MV enhanced survival of measles-immune mice. *A,* Kaplan Meier survival curves of mice given different treatments: saline, uninfected MSC, 10^5 $TCID_{50}$ naked MV-NIS, or 10^5 MV-NIS–infected MSC (MOI, 4.0, ~60% infection) in measles naïve mice (-Ab) or measles-immune mice (+Ab, 100 EU/mouse). *B,* immunohistochemical staining for measles-nucleocapsid (MV-N) protein (*blue staining*, site of viral gene expression) and CD68-positive macrophages (*brown/red staining*). Arrows, corresponding necrotic area in the tumor with minimal MV-N staining but strong CD68 staining. *Scale bars,* 500 μm.

carriers. In the case of MV, infection of a nontransformed cell such as MSC required larger amounts of virus (high MOI; MOI, 4.0) to obtain significant numbers (60%) of infected cells. Also, the clinical protocol incorporating cell carriers becomes more complex as it may involve harvest of autologous cells from the patients, expansion of the cells, and preloading of the cells with virus in a GLP cell processing facility. In addition, the trafficking profile of the cell carrier needs to be taken into consideration. *Ex vivo* expanded cells such as T cells, MSC, and dendritic cells tend to arrest in the lungs, liver, and spleen after intravascular infusion in experimental animals and humans (21, 25, 35, 36), although Power and Bell (37) recently determined that leukemic cell carriers were not so readily trapped in the lung vasculature and could deliver oncolytic vesicular stomatitis virus to tumors.

Autologous T cells, irradiated tumor cells, bone marrow–derived MSC, dendritic cells, and endothelial progenitor cells have been used to deliver oncolytic viruses to tumor xenografts (38). Coukos et al. (39) first showed the feasibility of using a human ovarian teratocarcinoma line PA-1 cell line for HSV-1716 virotherapy of ovarian cancer. PA-1 cells were preirradiated at 20 Gy before herpes simplex virus infection, after which cells were injected i.p. into athymic mice with peritoneal ovarian tumors. Irradiated PA-1 cells colocalized with tumor xenografts to result in significant enhancement in survival of tumor-bearing mice compared with nontreated controls or virus alone. Hamada et al. (40) were among the first to show that cell carriers can protect oncolytic viruses from neutralizing antiviral antibodies. Tumor cell carriers (A549 lung carcinoma) infected with a conditionally replicating adenovirus were irradiated before direct intratumoral injection into subcutaneous ovarian tumors in immunized syngeneic mice. Interestingly, treatment of virus-immune mice with cell carriers resulted in superior efficacy and complete tumor regressions compared with nonimmunized mice. Hamada et al. (40) suggested that superior antitumor activity could be due to induction of antiadenoviral and antitumoral CTL responses in the preimmunized animals. Bone marrow–derived MSC have been used successfully for delivery of oncolytic adenoviruses for the treatment of ovarian cancer or glioma xenografts (22, 24). They showed that mesenchymal progenitor cells infected by RGD displaying adenoviral vector homed to preestablished ovarian tumor nodules and extended the survival of tumor-bearing mice, although the feasibility of MSC to overcome antiviral antibodies was not addressed.

Due to previous debulking surgeries, ovarian cancer patients typically have extensive amounts of adhesions that could significantly hinder i.p. distribution of the virus after i.p. delivery. In addition, fluids injected into the peritoneal cavity rapidly drain of the cavity via the diaphragmatic stomata into the lymphatics, and from the mediastinal lymph node into the vascular system (41, 42). In contrast, i.p. administered MSC home to and localize on ovarian nodules in the peritoneal cavity of mice. Indeed, abundant MSC were seen "covering" the omental tumor nodules with minimal MSC in the omentum. In nontumor-bearing mice, i.p. injected MSC trafficked to and localized on the omentum instead. The omentum is an extension of the mesothelium that becomes drawn out and folded on itself during development and contains abundant milky spots, which consist predominantly of resident peritoneal macrophages (42, 43). Cancer cells injected i.p. into experimental animals preferentially home to, infiltrate, and engraft at the omentum (44, 45). As such, it is ideal that MSC appear to have a tropism for the omentum and tumor nodules, thus improving virus delivery to the tumor cells. The mechanism(s) that determines MSC tropism for tumors have not been fully elucidated, but it is clear

that signaling molecules produced by the tumor cells (e.g., stromal cell–derived growth factor SDF-1, monocyte chemoattractant protein MCP-1, vascular growth factor) and adhesion molecules (e.g., ICAM-1, integrins, and L-selectin) contribute to MSC tumor homing and engraftment (46–48).

Immunohistochemical staining revealed areas of MV gene expression in tumors from MV-NIS–treated (-Ab), MV/MSC–treated (-Ab), and MV/MSC–treated (+Ab) animals but not in tumors from MV-NIS–treated (+Ab) mice, confirming that the superior survival of mice required active viral replication and gene expression. Uninfected MSC did not have antitumor activity. Abundant infiltrates of CD68-positive macrophages were found in the measles-infected areas/tumors but minimal in uninfected tumors. The role of macrophages in the measles-infected tumors remains to be determined. They could be phagocytic macrophages whose role is to clear up nonviable virus-infected tumor cells as indicated by necrotic areas with negative/minimal MV-N staining but abundant CD68 staining. On the other hand, there were also areas where MV-N and CD68 staining overlapped. Chiocca and colleagues (49) proposed that CD68 macrophages, as part of the host innate immune response, inhibit virotherapy by restricting the intratumoral spread of oncolytic viruses. They have elegantly shown that addition of cyclophosphamide, an immunosuppressive agent, to oncolytic herpes virotherapy resulted in decreased numbers of infiltrating CD68 macrophages, increased intratumoral viral replication, and superior survival of mice (50). Certainly, research into optimal ways to combine cyclophosphamide with measles virotherapy in ovarian caner is needed; for example, the timing of drug administration is important as cyclophosphamide (an alkylating agent) may negatively impact the viability of cell carriers.

In contrast to studies using vaccinia or adenoviruses (24, 51), we did not observe an enhancement in the oncolytic activity of MV when using cell carriers compared with free virus in measles-naïve mice. Measles virus–infected MSC did not produce a significant amount of progeny virus; this is expected as MV replication is significantly lower in nontransformed cells than in cancer cells (13, 52). Hence, in the case of MV, it is likely that virus transfer from the MSC carriers to tumor occurred predominantly via heterofusion between the cell carrier and the tumor cells, rather than release of viral progeny. Data from our study also indicated that hemagglutinin-and fusion-induced intercellular fusion is much more resistant (32-fold) to the inhibitory effects of antimeasles antibodies. As such, at 69 EU/mL of measles-immune serum, cell-to-cell fusion was able to occur, whereas virus-to-cell fusion was evident only at 2 EU/mL of the serum. This observation bodes well for the use of virus-infected cell carriers as a possible means to circumvent antiviral antibodies in measles virotherapy.

Disclosure of Potential Conflicts of Interest

S.J. Russell and K.W. Peng are named inventors on patents owned by Mayo Clinic regarding oncolytic measles that have been licensed to a biotechnology company (NISCO).

Acknowledgments

We thank the Mayo Clinic Women's Cancer Program (Drs. Kimberly Kalli and Viji Shridhar) for the ascites samples and cell lines and Dr. Bakhos A. Tannous (Harvard Medical School, Cambridge, MA) for the kind gift of Gaussia luciferase expression plasmid.

References

1. Jemal A, Siegel R, Ward E, et al. Cancer statistics, 2008. CA Cancer J Clin 2008;58:71–96.
2. Badgwell D, Bast RC, Jr. Early detection of ovarian cancer. Dis Markers 2007;23:397–410.
3. Fung-Kee-Fung M, Oliver T, Elit L, et al. Optimal chemotherapy treatment for women with recurrent ovarian cancer. Curr Oncol Rep 2007;14:195–208.
4. Rocconi RP, Numnum TM, Stoff-Khalili M, et al. Targeted gene therapy for ovarian cancer. Curr Gene Ther 2005;5:643–53.
5. Kimball KJ, Numnum TM, Rocconi RP, Alvarez RD. Gene therapy for ovarian cancer. Curr Oncol Rep 2006;8:441–7.
6. Agarwal R, Linch M, Kaye SB. Novel therapeutic agents in ovarian cancer. Eur J Surg Oncol 2006;32:875–86.
7. Han ES, Monk BJ. Bevacizumab in the treatment of ovarian cancer. Expert Rev Anticancer Ther 2007;7:1339–45.
8. Chu CS, Kim SH, June CH, Coukos G. Immunotherapy opportunities in ovarian cancer. Expert Rev Anticancer Ther 2008;8:243–57.
9. Russell SJ, Peng KW. Viruses as anticancer drugs. Trends Pharmacol Sci 2007;28:326–33.
10. Peng KW, TenEyck CJ, Galanis E, et al. Intraperitoneal therapy of ovarian cancer using an engineered measles virus. Cancer Res 2002;62:4656–62.
11. Myers R, Greiner S, Harvey M, et al. Oncolytic activities of approved mumps and measles vaccines for therapy of ovarian cancer. Cancer Gene Ther 2005;12:593–9.
12. Anderson BD, Nakamura T, Russell SJ, Peng KW. High CD46 receptor density determines preferential killing of tumor cells by oncolytic measles virus. Cancer Res 2004;64:4919–26.
13. Ong HT, Timm MM, Greipp PR, et al. Oncolytic measles virus targets high CD46 expression on multiple myeloma cells. Exp Hematol 2006;34:713–20.
14. Bjorge L, Hakulinen J, Wahlstrom T, Matre R, Meri S. Complement-regulatory proteins in ovarian malignancies. Int J Cancer 1997;70:14–25.
15. Committee RDA Recombinant DNA Advisory Committee Meeting, U.S. Department of Health and Human Services, Public Health Service, National Institutes of Health, June 20-21, 2002. Protocol #0201-523: Phase I trial of intraperitoneal administration of an attenuated strain (Edmonston strain) of measles virus, genetically modified to produce carcinoembryonic antigen, in patients with recurrent ovarian cancer. Hum Gene Ther 2002;13:2220–2.
16. Galanis E, Hartmann LC, Cliby W, et al. Phase I trial of intraperitoneal (IP) administration of a measles virus (MV) derivative expressing the human carcinoembryonic antigen (CEA) in ovarian cancer patients. J Clin Oncol 2006;24:5028.
17. Raykov Z, Balboni G, Aprahamian M, Rommelaere J. Carrier cell-mediated delivery of oncolytic parvoviruses for targeting metastases. Int J Cancer 2004;109:742–9.
18. Thorne SH, Negrin RS, Contag CH. Synergistic antitumor effects of immune cell-viral biotherapy. Science 2006;311:1780–4.
19. Power AT, Wang J, Falls TJ, et al. Carrier cell-based delivery of an oncolytic virus circumvents antiviral immunity. Mol Ther 2007;15:123–30.
20. Iankov ID, Blechacz B, Liu C, et al. Infected cell carriers: a new strategy for systemic delivery of oncolytic measles viruses in cancer virotherapy. Mol Ther 2007;15:114–22.
21. Ong HT, Hasegawa K, Dietz AB, Russell SJ, Peng KW. Evaluation of T cells as carriers for systemic measles virotherapy in the presence of antiviral antibodies. Gene Ther 2007;14:324–33.
22. Sonabend AM, Ulasov IV, Tyler MA, et al. Mesenchymal stem cells effectively deliver an oncolytic adenovirus to intracranial glioma. Stem Cells 2008;26:831–41.
23. Raykov Z, Grekova S, Galabov AS, et al. Combined oncolytic and vaccination activities of parvovirus H-1 in a metastatic tumor model. Oncol Rep 2007;17:1493–9.
24. Komarova S, Kawakami Y, Stoff-Khalili MA, Curiel DT, Pereboeva L. Mesenchymal progenitor cells as cellular vehicles for delivery of oncolytic adenoviruses. Mol Cancer Ther 2006;5:755–66.
25. Peng KW, Dogan A, Vrana J, et al. Tumor-associated macrophages infiltrate plasmacytomas and can serve as cell carriers for oncolytic measles virotherapy of disseminated myeloma. Am J Hematol 2009;84:401–7.
26. Kidd S, Spaeth E, Klopp A, et al. The (in) auspicious role of mesenchymal stromal cells in cancer: be it friend or foe. Cytotherapy 2008;10:657–67.
27. Giordano A, Galderisi U, Marino IR. From the laboratory bench to the patient's bedside: an update on clinical trials with mesenchymal stem cells. J Cell Physiol 2007;211:27–35.
28. Peng KW, Facteau S, Wegman T, O'Kane D,

Russell SJ. Non-invasive *in vivo* monitoring of trackable viruses expressing soluble marker peptides. Nat Med 2002;8:527–31.

29. Dingli D, Peng KW, Harvey ME, et al. Image-guided radiovirotherapy for multiple myeloma using a recombinant measles virus expressing the thyroidal sodium iodide symporter. Blood 2004;103:1641–6.

30. Hewett JW, Tannous B, Niland BP, et al. Mutant torsinA interferes with protein processing through the secretory pathway in DYT1 dystonia cells. Proc Natl Acad Sci U S A 2007;104:7271–6.

31. Tannous BA, Kim DE, Fernandez JL, Weissleder R, Breakefield XO. Codon-optimized Gaussia luciferase cDNA for mammalian gene expression in culture and *in vivo*. Mol Ther 2005;11: 435–43.

32. Niewiesk S, Schneider-Schaulies J, Ohnimus H, et al. CD46 expression does not overcome the intracellular block of measles virus replication in transgenic rats. J Virol 1997;71:7969–973.

33. Vincent S, Tigaud I, Schneider H, et al. Restriction of measles virus RNA synthesis by a mouse host cell line: *trans*-complementation by polymerase components or a human cellular factor (s). J Virol 2002;76:6121–30.

34. Qiao J, Wang H, Kottke T, et al. Loading of oncolytic vesicular stomatitis virus onto antigen-specific T cells enhances the efficacy of adoptive T-cell therapy of tumors. Gene Ther 2008;15: 604–16.

35. Read EJ, Keenan AM, Carter CS, Yolles PS, Davey RJ. *In vivo* traffic of indium-111-oxine labeled human lymphocytes collected by automated apheresis. J Nucl Med 1990;31: 999–1006.

36. Hakkarainen T, Sarkioja M, Lehenkari P, et al. Human mesenchymal stem cells lack tumor tropism but enhance the antitumor activity of oncolytic adenoviruses in orthotopic lung and breast tumors. Hum Gene Ther 2007;18:627–41.

37. Power AT, Bell JC. Cell-based delivery of oncolytic viruses: a new strategic alliance for a biological strike against cancer. Mol Ther 2007;15: 660–5.

38. Russell SJ, Peng KW. The utility of cells as vehicles for oncolytic virus therapies. Curr Opin Mol Ther 2008;10:380–6.

39. Coukos G, Makrigiannakis A, Kang EH, et al. Use of carrier cells to deliver a replication-selective herpes simplex virus-1 mutant for the intraperitoneal therapy of epithelial ovarian cancer. Clin Cancer Res 1999;5:1523–37.

40. Hamada K, Desaki J, Nakagawa K, et al. Carrier cell-mediated delivery of a replication-competent adenovirus for cancer gene therapy. Mol Ther 2007;15:1121–8.

41. Abu-Hijleh MF, Habbal OA, Moqattash ST. The role of the diaphragm in lymphatic absorption from the peritoneal cavity. J Anat 1995;186: 453–67.

42. Doherty NS, Griffiths RJ, Hakkinen JP, Scampoli DN, Milici AJ. Post-capillary venules in the "milky spots" of the greater omentum are the major site of plasma protein and leukocyte extravasation in rodent models of peritonitis. Inflamm Res 1995;44:169–77.

43. Krist LF, Eestermans IL, Steenbergen JJ, et al. Cellular composition of milky spots in the human greater omentum: an immunochemical and ultrastructural study. Anat Rec 1995;241: 163–74.

44. Tsujimoto H, Hagiwara A, Shimotsuma M, et al. Role of milky spots as selective implantation sites for malignant cells in peritoneal dissemination in mice. J Cancer Res Clin Oncol 1996;122:590–5.

45. Lopes Cardozo AM, Gupta A, Koppe MJ, et al. Metastatic pattern of CC531 colon carcinoma cells in the abdominal cavity: an experimental model of peritoneal carcinomatosis in rats. Eur J Surg Oncol 2001;27:359–63.

46. Karp JM, Leng Teo GS. Mesenchymal stem cell homing: the devil is in the details. Cell Stem Cell 2009;4:206–16.

47. Spaeth E, Klopp A, Dembinski J, Andreeff M, Marini F. Inflammation and tumor microenvironments: defining the migratory itinerary of mesenchymal stem cells. Gene Ther 2008;15: 730–8.

48. Fox JM, Chamberlain G, Ashton BA, Middleton J. Recent advances into the understanding of mesenchymal stem cell trafficking. Br J Haematol 2007;137:491–502.

49. Chiocca EA. The host response to cancer virotherapy. Curr Opin Mol Ther 2008;10:38–45.

50. Fulci G, Breymann L, Gianni D, et al. Cyclophosphamide enhances glioma virotherapy by inhibiting innate immune responses. Proc Natl Acad Sci U S A 2006;103:12873–8.

51. Thorne SH, Contag CH. Integrating the biological characteristics of oncolytic viruses and immune cells can optimize therapeutic benefits of cell-based delivery. Gene Ther 2008;15: 753–8.

52. Peng KW, Ahmann GJ, Pham L, et al. Systemic therapy of myeloma xenografts by an attenuated measles virus. Blood 2001;98:2002–7.